Supplemental Data

for

Li et al,

A *Pole*^{P286R} mouse model of endometrial cancer recapitulates high mutational burden and immunotherapy response

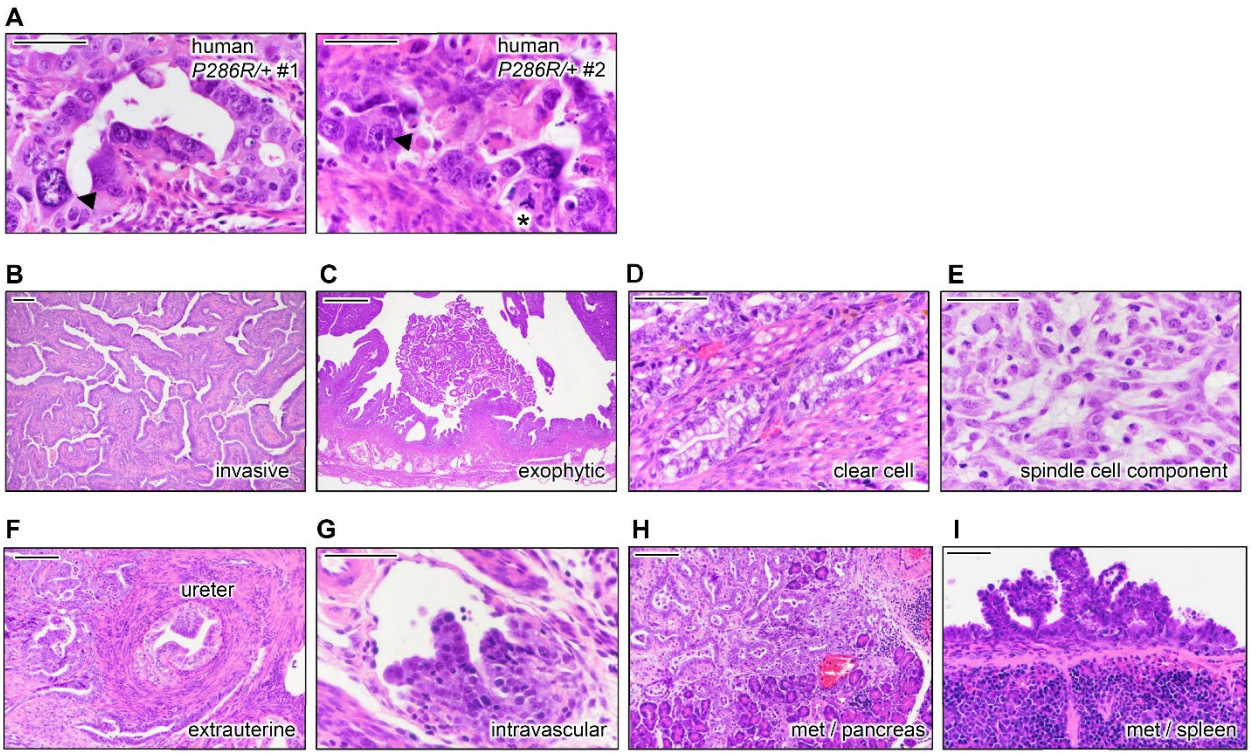

Figure S1. Histologic features of *Pole*^{P286R}/+ endometrial cancers. A) Two human *POLE*^{P286R}/+ endometrial cancers identified by exon 9 Sanger sequencing. B-F) Various histologic patterns in *Pole*^{P286R}/+ mouse tumors. B) Highly invasive endometrioid adenocarcinoma that did not form glands. C) Exophytic growth pattern. D) Clear cell pattern. E) Spindle cell component consistent with carcinosarcoma. F-I) Patterns and extent of invasion. F) Peri-ureteral invasion. G) Lymphovascular space invasion. H) Metastasis to pancreas. I) Metastasis to splenic capsule. Bars A, D, E, G=50 microns; B, F, H, I=100 microns; C=500 microns.

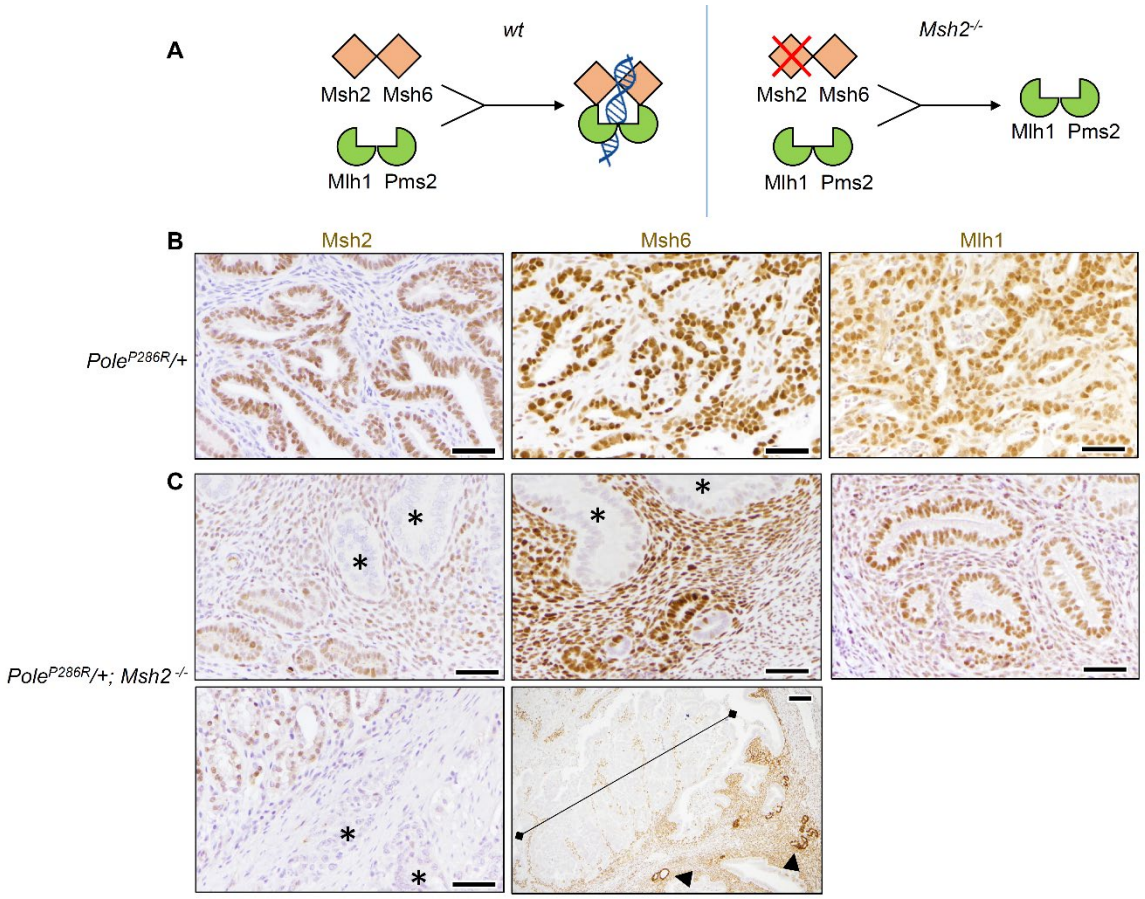

Figure S2. Validation of Msh2 inactivation by IHC against MMR components. A) Schematic of MMR factors. Msh2/Msh6 form a dimer where inactivation of either component leads to destabilization/degradation of both components. B) *Pole*^{P286R}/+ tumors, no dMMR as evidenced by retained expression of MMR factors Msh2, Msh6, and Mlh1. C) *Pole*^{P286R}/+; *Msh2*$^{-/-}$ uteri at euthanasia due to tumor-burden criteria (230-288 days of age) exhibit mosaic loss of Msh2/Msh6 (asterisks) as expected, with complete loss in invasive cancers (bottom panels). Bottom panels are of a metastasis to the colon (left) and a primary endometrial cancer (right). Normal colonic epithelium (upper left side) expresses Msh2, whereas metastatic glands invading colon wall (lower right, asterisks) do not. The endometrial cancer (demarcated with a line) shows loss of expression (but retention in rare normal glands, arrowheads). Bar=50 microns in all panels except lower Msh6 panel, bar=100 microns.

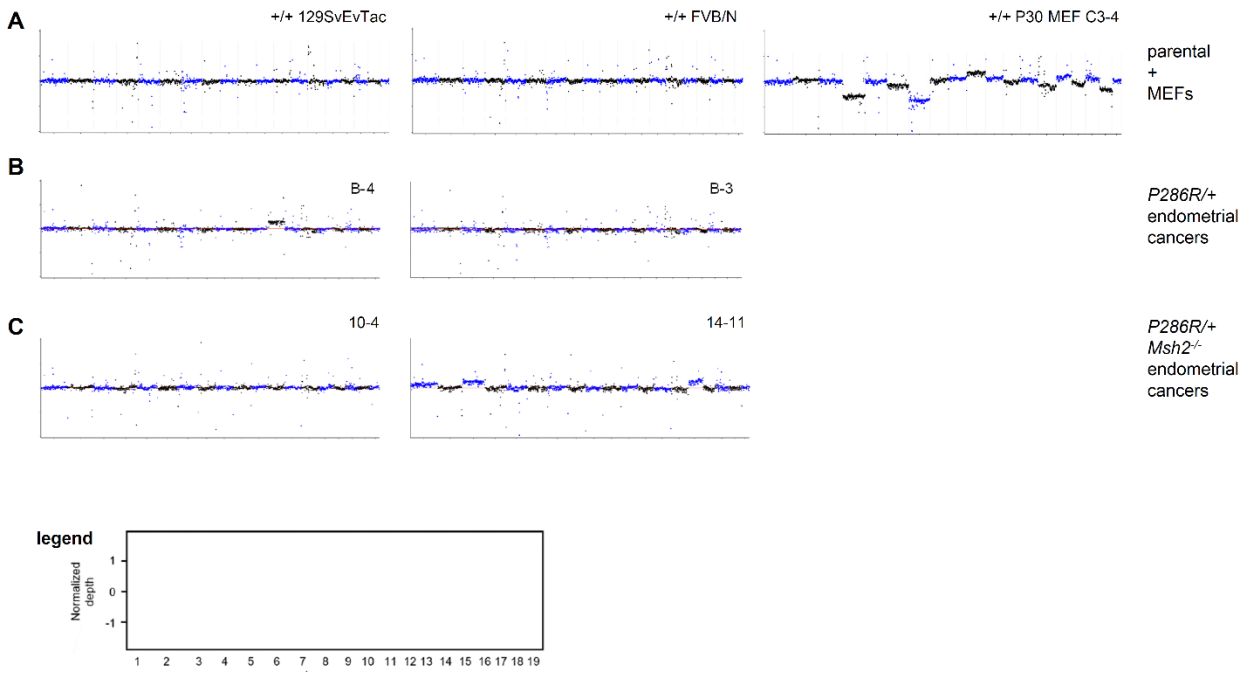

Figure S3. Copy number plots from WGS data (representative individual samples). For each sample y-axis represents normalized depth (log_2(depth/median depth across genome)). The x-axis represents position among the 19 autosomes as illustrated. A) Control samples including parental 129SvEvTac and FVB mouse DNA and +/+ passage 30 mouse embryo fibroblast line. The analysis shows that some large-scale chromosomal instability occurs during immortalization and serial passage of wild-type fibroblasts. B) Two *Pole*^{P286R}/+ primary tumors from different mice (additional examples to tumor shown in Figure 4C). C) Two additional *Pole*^{P286R}/+; *Msh2*$^{-/-}$ primary tumors (additional examples to tumor shown in Figure 4C). The analysis shows that neither *Pole*^{P286R} by itself or together with *Msh2* deficiency results in prominent large-scale chromosomal instability; only small numbers of events are detected.

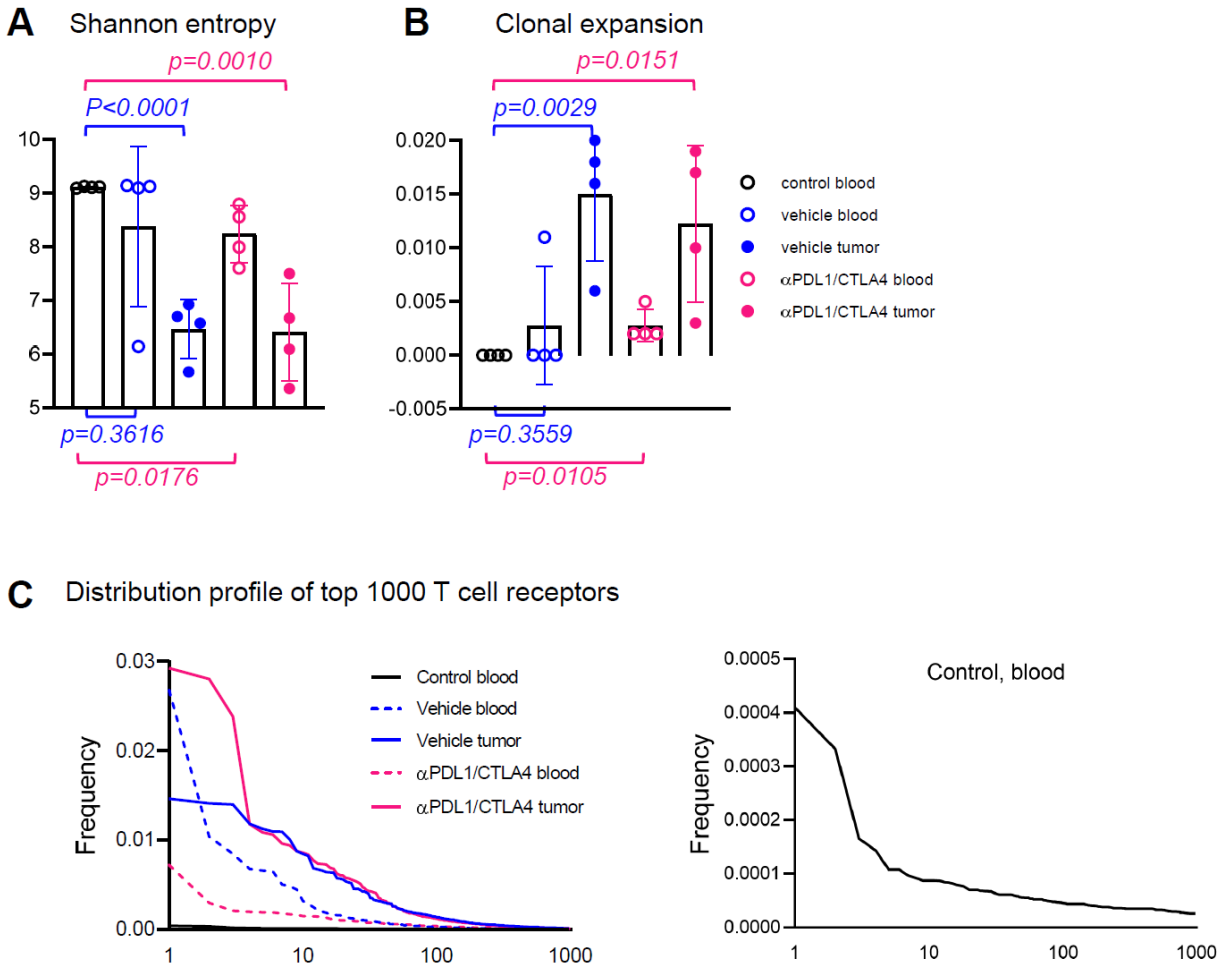

Figure S4. Degree of T cell receptor diversity and clonal expansion. A) Shannon entropy index assess T cell receptor diversity. The higher entropy index reflects higher TCR diversity, n=4. B) Clonality as a measure of how evenly TCR sequences are distributed. Clonality ranges from 0.0 to 1.0, where 0.0 represents a completely even sample and 1.0 represents a sample with a single dominant clone, n=4 (1). C) Distribution profile of top 1000 T cell receptor sequences in each group, x-axis=TCR clone number, from top 1 to top 1000. Since there is no T cell receptor expansion in peripheral blood from control mice without tumor grafts, T cell receptor frequency of control blood is also shown separately on right.

1. Immunoseq. https://clients.adaptivebiotech.com/assets/downloads/immunoSEQ_AnalyzerManual.pdf. Accessed March 8, 2020.